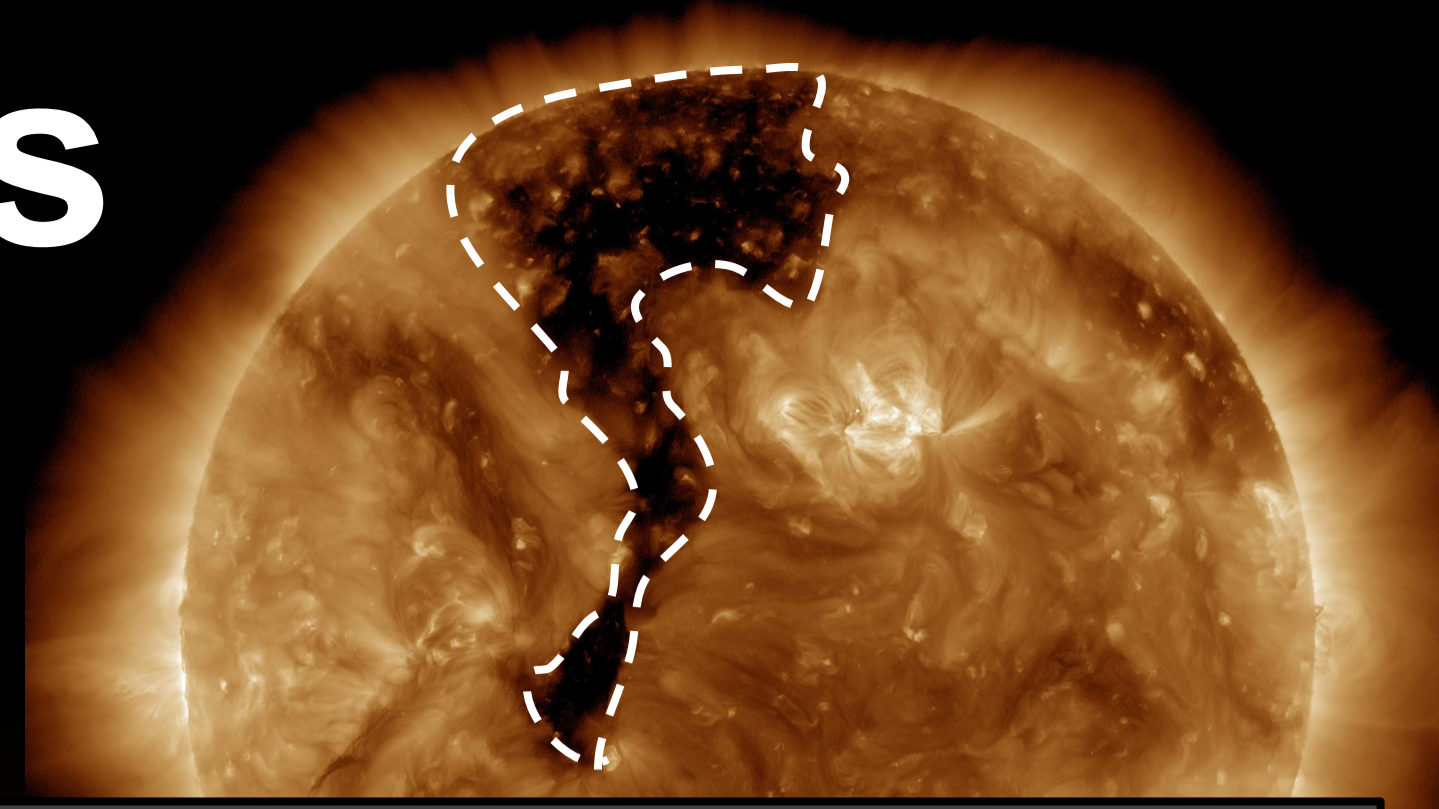


SEARCH: SEgmentation of Active Regions and Coronal Holes

Linnea M. Wolniewicz^{1,2}, Benoit Tremblay^{1,2,3}, Ajay Kumar Tiwari⁴, Andong Hu⁵, Michael Kirk^{6,7}, Silvina Guidoni⁸, Brent Smith⁹, Matthew Penn¹⁰, Tanmoy Samanta⁷

¹CU Boulder, USA - ²Laboratory for Atmospheric & Space Physics, USA - ³National Solar Observatory, USA - ⁴Centrum Wiskunde & Informatica, NL - ⁵CIRES, USA - ⁶ASTRA, USA - ⁷NASA Goddard Space Flight Center, USA - ⁸American University, USA - ⁹Johns Hopkins Applied Physics Laboratory, USA - ¹⁰NVIDIA, USA



1. Introduction to the Sun's Coronal Holes

- Solar coronal holes (CH)** are dark regions observed in images of the Sun taken in extreme ultraviolet (EUV) and soft X-ray wavelengths (**Figure 1**). CHs correspond to magnetic field lines (represented with white lines in **Figure 1**) that originate at the Sun and extend to interplanetary space (*open field*).
- Polar regions of the Sun are of special interest for space weather because they are the sources of high speed solar wind towards the Earth and other planets [1, 2, 3], but they remain elusive to the current constraints of solar imagery. **Indirect methods are needed for understanding the polar environment, including polar CHs.** Polar magnetic fields are used to forecast upcoming solar magnetic activity cycles [4, 5].
- The identification of CHs has been done traditionally with intensity-based thresholding methods applied to Sun images. Recent advances include supervised machine learning (ML) methods [6, 7].
- In this work, we attempt to **automatically identify both CHs and active regions (ARs; Figure 1)**, typically associated with closed, confined magnetic field lines. Solar flares and coronal mass ejections, the main drivers of space weather, originate in ARs.
- We address the identification of CHs and ARs in EUV maps using unsupervised learning (clustering and convolutional neural networks), i.e. without the use of models or databases and the biases they may have.** We also experiment with *transfer learning* techniques when training convolutional neural networks (encoder+decoder).

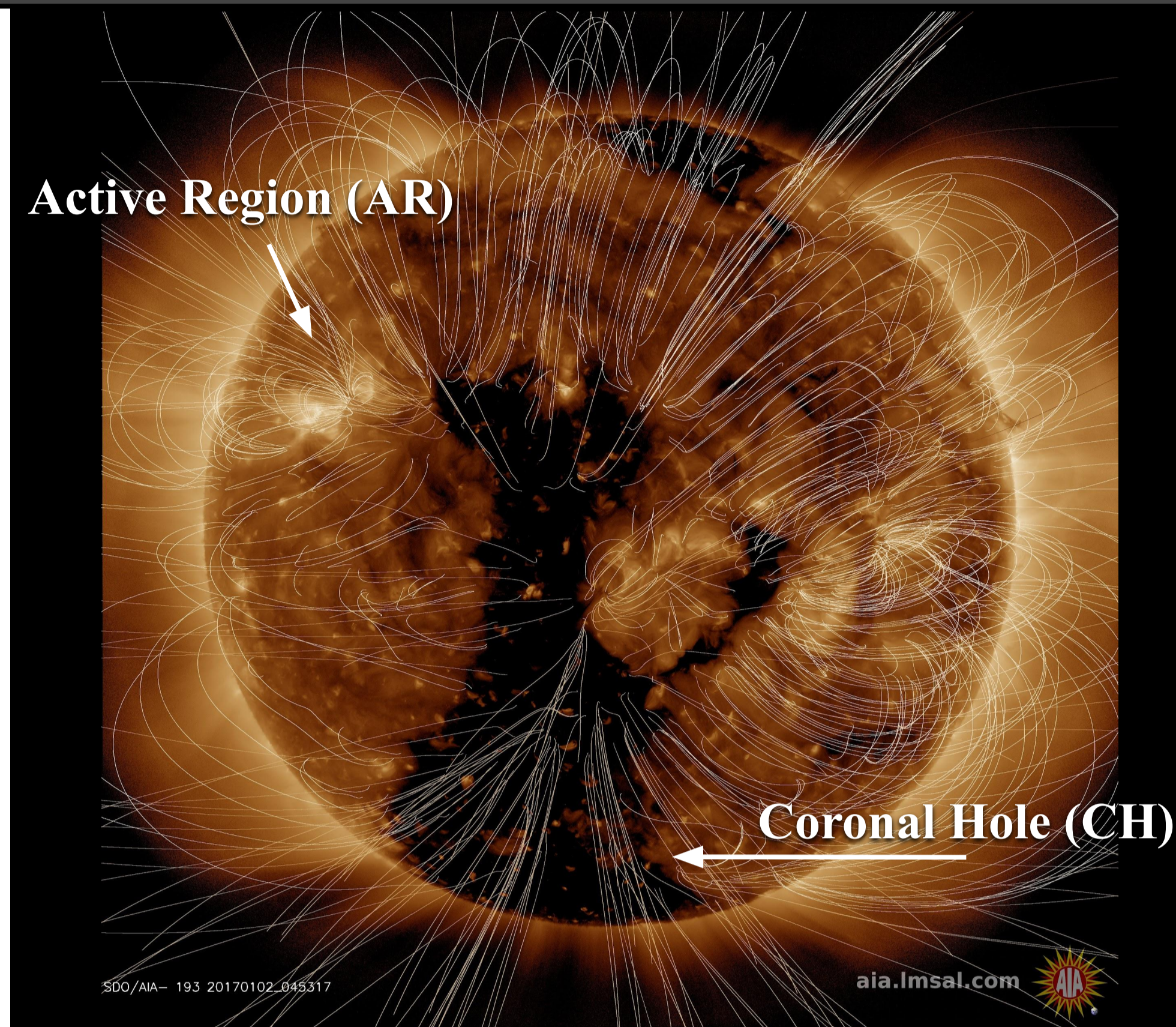


Figure 1: Full-disk image of the Sun captured at a EUV wavelength of 193Å by the Atmospheric Imaging Assembly (AIA) onboard the Solar Dynamics Observatory (SDO).

2. Synchronic Maps

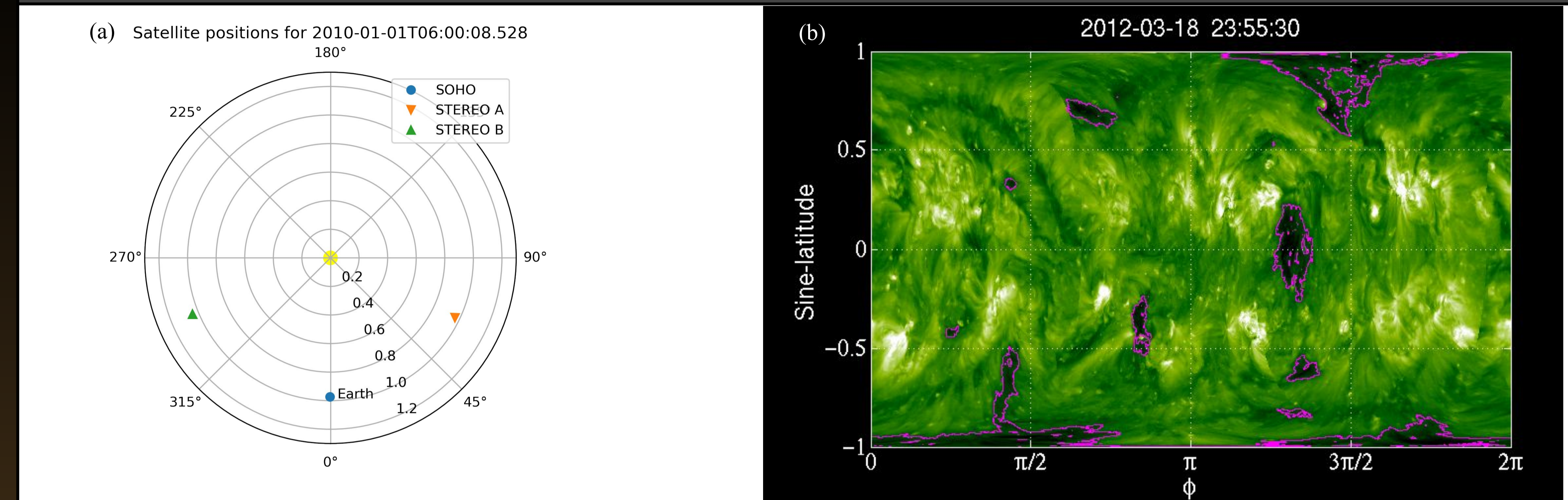


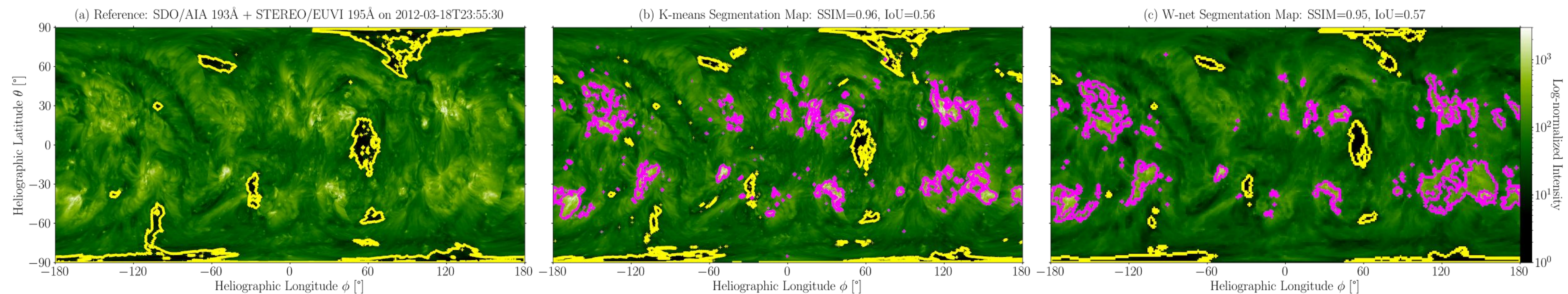
Figure 2: (a) Position of the Solar and Heliospheric Observatory (SoHO) and Solar Terrestrial Relations Observatory Ahead (STEREO-A) & Behind (STEREO-B) satellites on 2010-05-10. (b) **Synchronic maps:** The combination of simultaneous multi-stereoscopic EUV images of the Sun (captured at 195Å by SDO, and STEREO-A & -B). This image is a single-wavelength synchronic map from the [Predictive Science Inc. \(PSI\) database](#), with coronal holes outlined in yellow. **PSI CH detections using the EZSEG region-growing method** (not machine learning) [8] will be used as **reference images** to evaluate unsupervised learning methods.

3. Using Unsupervised Machine Learning for the Segmentation of (Polar) Coronal Holes and Active Regions in Synchronic Maps

CH detection methods are limited to existing catalogues and methods as there is no objective way to define CH boundaries. The intersection over union metric (IoU) and the structural similarity index (SSIM) were used to measure the accuracy and the similarity of unsupervised learning with respect to existing CH detections.

Figure 3: Comparisons of three CH detection methods using single-wavelength synchronic maps from the [Predictive Science Inc. \(PSI\) database](#) (colored background). **CHs are shown in yellow and magnetically active regions (ARs) in magenta.**

- (a) **PSI CH detections using the EZSEG region-growing-style method** (not machine learning!) [8]. Reference to evaluate IoU and SSIM of unsupervised learning methods.
- (b) **K-means clustering technique** trained to identify 6 clusters, i.e. the optimal number computed by the Elbow method [9]. Average SSIM=0.96, IoU=0.60.
- (c) **W-net convolutional neural network** [10, 11], with a fully-connected conditional random field (CRF) mask to smooth the segmentation maps. Input images and reference CH masks were downsampled by a factor of 10 in each spatial dimension for memory considerations. Average SSIM=0.95, IoU=0.53.



4. Science Application: Correlation between Polar Magnetic Field Strength and Coronal Hole Area

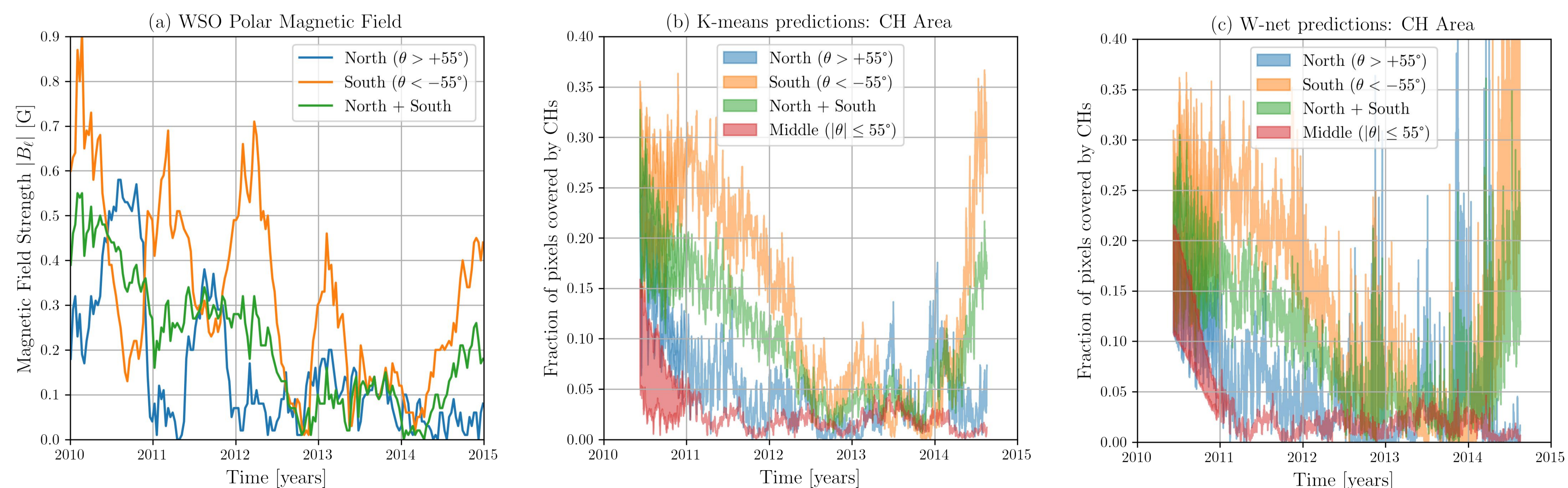


Figure 4: Correlation between magnetic field strength at the Sun's poles (latitude $|\theta| > 55^\circ$) and area of polar CHs (fraction of pixels that were labeled as CHs in the same time window). (a) Magnetic field strength from the [Wilcox Solar Observatory \(WSO\)](#). (b) Area of polar CHs computed using K-means. (c) Area of polar CHs computed using the W-net. For each pole, the lower curve assumes that there are no CHs where data is unavailable (lower limit) and the upper curve assumes that all unavailable data belong to CHs (upper limit). **Conclusion: CH size measurements appear to be a good proxy for long-term changes in polar fields, but more work is needed to causally link the two phenomena.**

5. Conclusion & Future Work

In conclusion:

- Unsupervised segmentations provides an **unbiased** way of identifying coronal holes and additionally active regions, two of the most important features for space weather applications.
- The coronal holes identified are consistent with the existing detections [8].
- Preliminary analysis of the magnetic field strength and the polar coronal hole area follows similar trend observed in previous studies [12].

Future work:

- Fully implement transfer learning techniques to improve W-net (in progress).
- Optimize the W-net convolutional neural network for solar images.
- Experiment with other unsupervised learning method: Bayesian Gaussian Mixture.
- Study the relationship between coronal hole area and geomagnetic activity at L1.
- Explore the relationship between the solar cycle and coronal hole area using EUV images captured by SoHO over a full 22-year magnetic cycle.

References

- | | | |
|--|---|--|
| [1] Nolte et al., 1976 | [5] Pesnell and Schatten, 2018 | [9] Joshi & Nalwade, 2013 |
| [2] Harvey and Sheeley, 1978 | [6] Illarionov & Tlatov, 2018 | [10] Xia & Kulis, 2017 |
| [3] Wang and Sheeley, 1990 | [7] Illarionov et al., 2020 | [11] Rajendrakumar Gare et al., 2020 |
| [4] Schatten et al., 1978 | [8] Caplan et al., 2016 | [12] Cranmer, S. R., 2009 |

Acknowledgements

This project was first conducted as part of the [NASA HelioHackweek 2020](#). The authors would like to thank their fellow SEARCH team members Emily Mason, Jake Strang, Jamie Staeben, and Luisa Capannolo for their participation, the organizers of HW20 at NASA and at the NASA Center for Climate Simulation, and the team at NVIDIA for their support.